Highly stable precursor solution containing ZnO nanoparticles for the preparation of ZnO thin film transistors

2010 Nanotechnology 21 295707

(http://iopscience.iop.org/0957-4484/21/29/295707)

IOP PUBLISHING NANOTECHNOLOGY

Nanotechnology **21** (2010) 295707 (7pp) doi:10.1088/0957-4484/21/29/295707

Highly stable precursor solution containing ZnO nanoparticles for the preparation of ZnO thin film transistors

Heh-Chang Huang and Tsung-Eong Hsieh[1]

Department of Materials Science and Engineering, National Chiao Tung University,
1001 Ta-Hsueh Road, Hsinchu, Taiwan 30010, Republic of China

E-mail: tehsieh@mail.nctu.edu.tw

Received 9 March 2010, in final form 24 May 2010
Published 5 July 2010
Online at stacks.iop.org/Nano/21/295707

Abstract

ZnO particles with an average size of about 5 nm were prepared via a sol–gel chemical route and the silane coupling agent, (3-glycidyloxypropyl)-trimethoxysilane (GPTS), was adopted to enhance the dispersion of the ZnO nanoparticles in ethyl glycol (EG) solution. A ZnO surface potential as high as 66 mV was observed and a sedimentation test showed that the ZnO precursor solution remains transparent for six months of storage, elucidating the success of surface modification on ZnO nanoparticles. The ZnO thin films were then prepared by spin coating the precursor solution on a Si wafer and annealing treatments at temperatures up to 500 °C were performed for subsequent preparation of ZnO thin film transistors (TFTs). Microstructure characterization revealed that the coalescence of ZnO nanoparticles occurs at temperatures as low as 200 °C to result in a highly uniform, nearly pore-free layer. However, annealing at higher temperatures was required to remove organic residues in the ZnO layer for satisfactory device performance. The 500 °C-annealed ZnO TFT sample exhibited the best electrical properties with on/off ratio $= 10^5$, threshold voltage $= 17.1$ V and mobility $(\mu) = 0.104\ \mathrm{cm^2\ V^{-1}\ s^{-1}}$.

1. Introduction

Transparent conductive oxides (TCOs) have attracted numerous research interests due to their wide applications as the conducting electrodes in flat panel displays (FPDs) [1], ultraviolet light emitting diodes (UV-LEDs) [2] and energy resource devices such as solar cells [3]. Presently indium tin oxide (ITO) is the most commonly seen TCO; however, its high cost, toxicity and the scarcity of the indium (In) element have called for ZnO-based materials as an alternative to TCOs. In addition to the similarity in optical and electrical properties to those of ITO, ZnO possesses the advantages of low cost, abundance, high stability and versatility in deposition processes [4]. Recently, the pursuit of a 'green' process and difficulties of the conventional photolithography process in large-area FPD fabrication have ignited the development of solution processes, also termed wet processes, for TCO films. In particular, the low-temperature, vacuum-free process draws a lot of attention due to its promising applications in flexible FPDs and energy resource products. For the solution process, organic electrode materials such as poly(3-hexylthiophene) (P3HT) [5] and dihexylquaterthiophene (DH4T) [6] have been widely studied; however, they have inferior stabilities in humid ambient. Such a deficiency does not apply to inorganic ZnO; nevertheless, the solution processes frequently encounter difficulties including undesired impurities and inferior film qualities which deteriorate the electrical properties of 'wet' ZnO layers. Further, post-annealing is an inevitable step for solution processes and the processing temperatures are usually high. To date, numerous studies have been conducted to solve these difficulties for the realization of solution processes. Okamura *et al* prepared a ZnO thin film transistor (TFT) by a solution process and found that the addition of an appropriate stabilizer may improve the ZnO/insulating layer interface roughness so as to increase the device mobility (μ) from 2.0×10^{-4} to $8.4 \times 10^{-3}\ \mathrm{cm^2\ V^{-1}\ s^{-1}}$ [7]. Sun *et al* prepared a self-assembly ZnO nanorod field-effect transistor and $\mu = 1.2\ \mathrm{cm^2\ V^{-1}\ s^{-1}}$ and on/off ratio $= 10^5$–10^6 were

---

[1] Author to whom any correspondence should be addressed.

achieved [8]. They ascribed the good device performance to the high ZnO film quality. A study on a flexible ZnO TFT utilizing a spin coating process with $\mu = 1.02 \times 10^{-3}$ cm^2 V^{-1} s^{-1} at temperatures as low as 150 °C was reported by Schneider *et al* [9]. Sun and Sirringhaus adopted butylamine as the stabilizer of ZnO nanorods in chloroform to fabricate ZnO TFT and $\mu = 0.61$ cm^2 V^{-1} s^{-1} and on/off ratio $= 3 \times 10^5$ were obtained at temperature = 230 °C [10]. Ong *et al* stabilized ZnO particles in methoxyethanol by ethanolamine and, with an annealing treatment at 500 °C, their device exhibited $\mu = 5.25$ cm^2 V^{-1} s^{-1} and on/off ratio $= 1.65 \times 10^5$ [11]. In addition to the efforts to solve the difficulties mentioned above, previous studies also indicated the preparation of ZnO particles with uniform sizes and highly stable precursor solutions with appropriate surface modification agents are essential for solution processes.

This study reports the synthesis of ZnO nanoparticles and their surface modification by a silane coupling agent to form a highly stable colloidal solution. The precursor solution was consequently applied to prepare ZnO thin films via spin coating for TFT device fabrication. The microstructures and optical properties of ZnO layers were characterized and their correlations to the electrical properties of ZnO TFT were discussed accordingly.

2. Experimental details

2.1. Materials

Zinc acetate dihydrate ($Zn(Ac)_2{\cdot}2H_2O$; purity = 99.6%) purchased from J T Baker, Ltd was adopted for ZnO precursor preparation. The solvents including absolute ethanol (purity = 99.5%), hexane (purity = 95%) and ethyl glycol (EG, purity = 99.5%) were supplied by Fluka, Seedchem and Scharlau Ltd, respectively. Lithium hydroxide monohydrate ($LiOH{\cdot}H_2O$; purity = 99%) obtained from TEDIA is the basic catalyst for synthesizing the ZnO nanoparticles. The surface modification agent, (3-glycidyloxypropyl)-trimethoxysilane (GPTS, purity = 97%), was provided by Lancaster Ltd. All reagents were used directly without further purification. 4″, n-type (100)Si wafers purchased from Swiftek, Ltd were used as the substrates for sample preparation.

2.2. Preparation of ZnO nanoparticles

The method for preparing ZnO nanoparticles and its modifications have been reported elsewhere [12, 13]. In a typical run, 2.2 g of $Zn(Ac)_2{\cdot}2H_2O$ was first dissolved in 150 ml boiling ethanol, refluxed at 80 °C in argon ambient, and then held at this temperature for 3 h under vigorous stirring. During this process, 90 ml of ethanol was removed by distillation. After cooling the above mixture down to 0 °C, 90 ml of 0.58 g $LiOH{\cdot}H_2O$ in ethanol solution was added into the mixture under vigorous stirring. The stock solution was stirred continuously at room temperature for another 2 h until the mixed solution became transparent. By adding 300 ml of hexane to the solution and subsequently removing the supernatant by centrifugation, nano-scale ZnO particles with an average size of about 5 nm could be obtained [14]. 50 ml of ethanol was added into the ZnO nanoparticles to re-suspend the ZnO nanoparticles in ethanol.

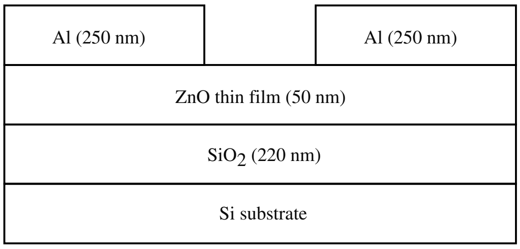

Figure 1. Cross-sectional view of the TFT device.

2.3. Surface modification of ZnO nanoparticles

In order to obtain a highly stable ZnO precursor solution, silane coupling agent, GPTS, was added to stabilize the ZnO nanoparticles in the ethyl glycol (EG) solvent within the procedures developed previously [14, 15]. First, 0.3 ml GPTS in 5 ml ethanol solution was added into the 150 ml as-synthesized ZnO nanoparticles in ethanol solution at 0 °C and a reaction for 2 h was allowed. Afterward, the mixture was stirred at room temperature for 24 h. After adding hexane, the GPTS-modified ZnO nanoparticles were obtained by centrifugally removing the supernatant.

2.4. Preparation of TFT devices

A 220 nm thick SiO_2 layer serving as the gate insulator was first grown on Si substrate via a wet oxidation process then modified by a UV ozone surface treatment for 15 min. An appropriate amount of GPTS-modified ZnO nanoparticles was added to EG solvent to form the precursor solution for spin coating on the SiO_2 layer at an initial coating rate = 500 rpm for 5 s followed by a terminal coating rate = 3000 rpm for 99 s. After the spin coating deposition, the ZnO thin films were formed by annealing at temperatures ranging from 200 to 500 °C for 2 h. Afterward, a 250 nm thick Al metal line serving as source and drain electrodes of TFT samples was deposited on the ZnO layer by e-beam evaporation to complete the device preparation. The cross-sectional view of the TFT sample is schematically shown in figure 1.

2.5. Microstructure and property characterization

Analytical results of the microstructure and optical properties of ZnO nanoparticles have been reported previously [14]. It was found that the average particle size is about 5 nm and the synthesized ZnO possesses typical wurtzite structure and abounds with lattice defects. In this work, analytical methods of microstructure and properties of GPTS-modified ZnO are described as follows. The absorption spectra of the ZnO thin films were recorded by a UV–vis spectrophotometer (Hitachi 3900H). The surface potential of the ZnO nanoparticles was measured by a zeta potential meter (Beckman Coulter Delsa™ Nano C Analyzer). Thermogravimetric analysis (TGA) using a TA Instruments Q500 TGA operating in a nitrogen (N_2) atmosphere at a heating rate of 10 °C min^{-1} was adopted to explore the thermal properties of GPTS-modified ZnO. Fourier-transform infrared (FT-IR) spectra of the ZnO thin films and ZnO nanoparticles before and after the surface

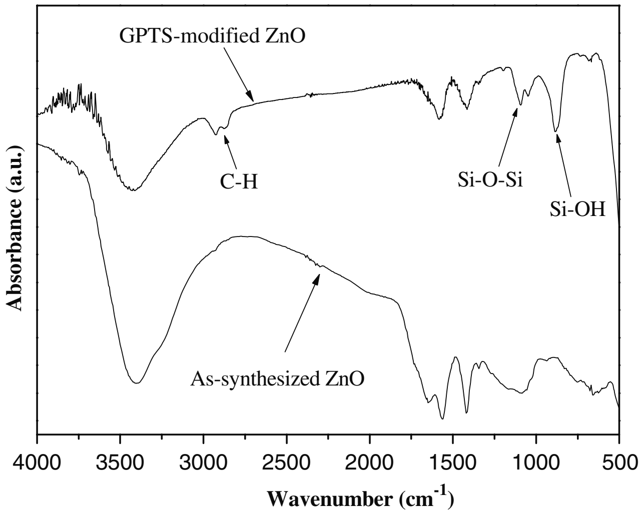

Figure 2. FT-IR spectra of as-synthesized and GPTS-modified ZnO nanoparticles.

modification by GPTS were characterized by a PerkinElmer spectrum 100 FT-IR spectrometer. The crystal structure of the ZnO thin films was characterized by an x-ray diffractometer (XRD, Rigaku TTRAX III) with Cu Kα radiation ($\lambda = 0.154$ nm) at a scan rate of 2° min^{-1}. The microstructure of the ZnO thin film was examined by a transmission electron microscope (TEM, Philips Tecnai 20) operating at 200 kV and a field-emission scanning electron microscope (FE-SEM, JEOL JSM-6700) operating at 15 kV. The electrical properties of the ZnO TFT devices were measured by a Keithley MODEL4200-SCS semiconductor characterization system and μ was calculated from the saturation region according to the formula [16]:

$$\mu = \frac{2LI_D}{C_i W(V_G - V_{th})^2} \qquad (1)$$

where C_i = gate capacitance per unit area, V_{th} = threshold voltage, W = channel width, L = channel length, I_D = drain current and V_G = gate voltage. In this work, $C_i = 1.57 \times 10^{-8}$ F cm^{-2}, $W = 0.1$ mm and $L = 2$ mm, respectively.

3. Results and discussion

3.1. Surface modification of ZnO nanoparticles

Silane coupling agent was added in order to stabilize the ZnO nanoparticles in EG solvent so as to obtain a highly stable ZnO precursor solution for subsequent device preparation via spin coating or an inkjet printing process. The reasons for choosing GPTS as the coupling agent of ZnO are its good compatibility with EG and the capability of the silane functional group to graft the ZnO nanoparticle surface so as to stabilize the ZnO nanoparticle in the EG solution. GPTS is a nonionic coupling agent with a silane functional group at one side that may graft the ZnO nanoparticle's surface and a carbon chain at the other side that provides the steric hindrance to disperse the ZnO nanoparticles in EG solution. Figure 2 shows the FT-IR spectra of as-synthesized ZnO and that subjected to surface modification by GPTS. The absorption bands at 1565 and 1420 cm^{-1} in both samples are assigned to the surface absorbed carboxylate anion complex [17] with the zinc center, which indicates the chemical absorption of the acetate group on the surface of the ZnO. The absorption band at 3400 cm^{-1} is ascribed to O–H vibration on the ZnO nanoparticle surface [18]. As to the GPTS-modified ZnO, the absorption band for Si–OH stretching vibration at 885 cm^{-1}, the Si–O–Si asymmetrical stretching vibration peak at 1122 cm^{-1} [19], and the saturated C–H absorption bands at 2948 and 2882 cm^{-1} emerge. This evidences the successful attachment of GPTS on ZnO nanoparticles.

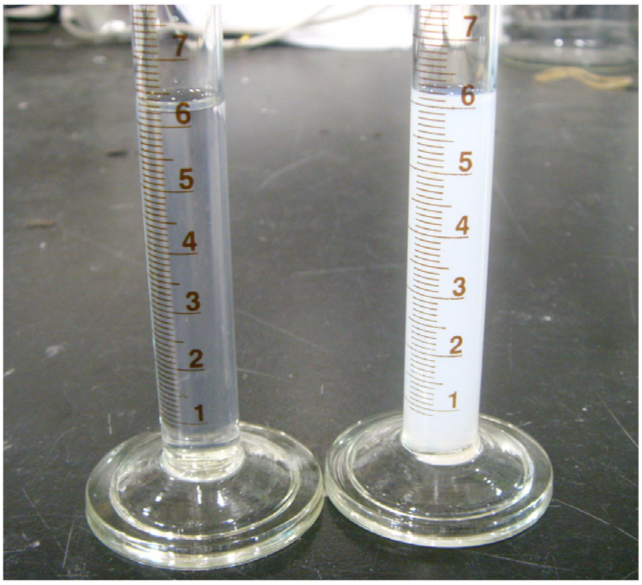

Figure 3. Sedimentation test result of precursor solutions containing the GPTS-modified ZnO nanoparticles and unmodified ZnO nanoparticles.

The zeta potential measurement indicated that, for GPTS-modified ZnO suspensions, the average surface potential is 66 mV whereas, for the ZnO solution without GPTS modification, the surface potential is about 27 mV. This indicates that GPTS is indeed an effective dispersive agent to stabilize the ZnO nanoparticles in EG and the surface charges on ZnO nanoparticles are positive prior to GPTS modification. After the surface modification, it is believed that GPTS may inhibit the absorption of the carboxylate anion complex on the ZnO nanoparticles so as to induce a drastic increase of the surface potential. It is known that strong chemisorption of GPTS on ZnO particles could prevent desorption during particle collision [20] and, with the steric hindrance effect and surface potential increment induced by GPTS modification, the good dispersion of the ZnO nanoparticles in EG is hence achieved.

A sedimentation test was performed by storing the ZnO precursor solutions, with and without GPTS modification, for six months and the result is presented in figure 3. It can be seen that the solution sample containing the GPTS-modified ZnO remains transparent and the sample without GPTS modification is opaque. In fact, opaqueness due to

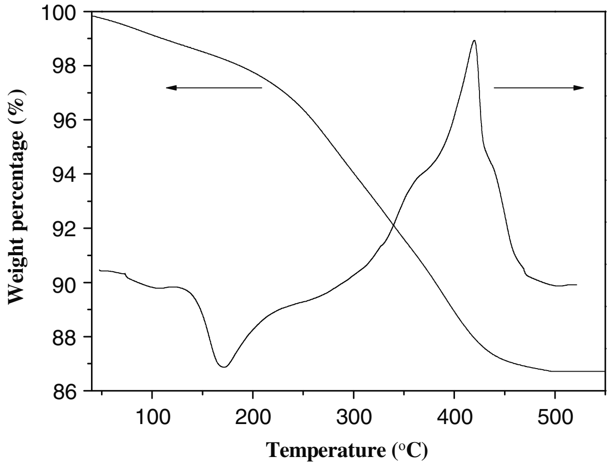

Figure 4. TGA/DTA spectra of GPTS-modified ZnO nanoparticles.

the aggregation of ZnO nanoparticles was observed in the sample without GPTS modification after one day's storage. This illustrates that GPTS could effectively stabilize the ZnO nanoparticles in EG solvent and it is feasible for various types of solution processes.

Figure 4 shows the TGA/DTA spectrum of GPTS-modified ZnO nanoparticles and it reveals that the O–H group on the ZnO nanoparticle's surface is eliminated between 150 and 170 °C [18] whereas GPTS is decomposed in the range of 370–430 °C. The char yield occurs at a temperature of about 500 °C, indicating that an annealing treatment at a temperature equal to or greater than 500 °C may be required to eliminate the hydroxyl group and GPTS residing on the ZnO nanoparticles if the precursor solution were intended to implant in the fabrication of ZnO TFT devices with satisfactory electrical properties.

3.2. *Characterization of ZnO thin films*

Figure 5 shows FT-IR spectra of as-deposited and ZnO thin films subjected to annealing at 200, 400 and 500 °C for 2 h, respectively. In comparison with the spectrum of as-deposited ZnO thin film, annealing at 200 °C causes a dramatic decrease of the absorption band at about 3400 cm^{-1}, which implies the elimination of hydroxyl groups on ZnO nanoparticles [18]. Saturated C–H absorption bands at 2948 and 2882 cm^{-1} of GPTS gradually diminish with a further increase of annealing temperature to 400 °C, indicating the decomposition of GPTS during annealing. Analytical results obtained by FT-IR are in good agreement with those obtained by TGA/DTA; its implication on the annealing temperature of the ZnO layer to achieve satisfactory TFT device performance will be shown in a later part of the discussion.

Figure 6(a) depicts the appearances of as-deposited and annealed ZnO thin films on glass substrate and figure 6(b) displays the UV–vis spectrum of annealed ZnO thin film. It illustrates the 150 nm thick ZnO thin film subjected to annealing at 500 °C for 2 h is highly transparent in the visible-light region (transmittance > 97.5%). This indicates that the ZnO precursor solution prepared in this work can also be applied to the preparation of fully transparent TFT devices.

Figures 7(a) and (b) present the top and cross-sectional SEM views of ZnO thin films subjected to annealing at 200 and 500 °C for 2 h, respectively. It can be readily seen that highly uniform, nearly pore-free ZnO thin films of about 50 nm in thickness are obtained. The cross-sectional SEM micrograph

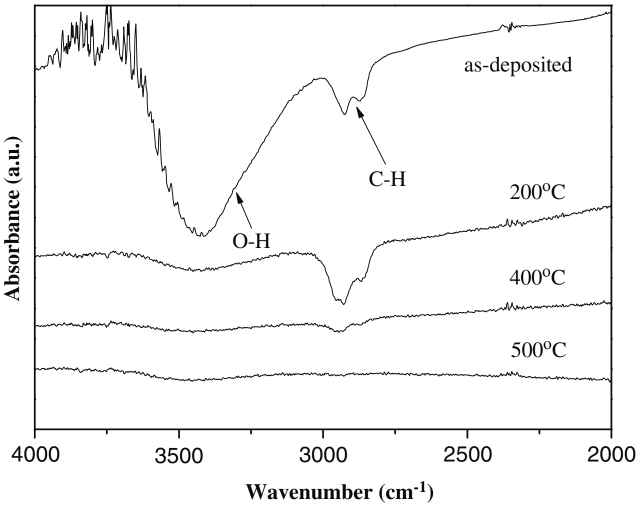

Figure 5. FT-IR spectra of as-deposited and annealed ZnO thin films subjected to annealing at 200, 400 and 500 °C for 2 h.

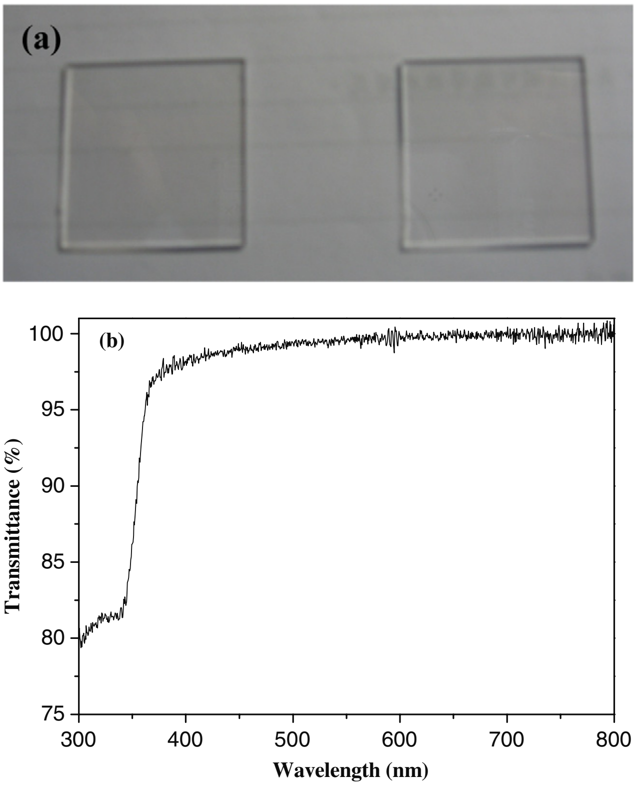

Figure 6. (a) The appearances of as-deposited (right) and annealed (left) ZnO thin films. (b) UV–vis spectrum of ZnO thin film subjected to annealing at 500 °C for 2 h. The thickness of the ZnO thin film is about 150 nm.

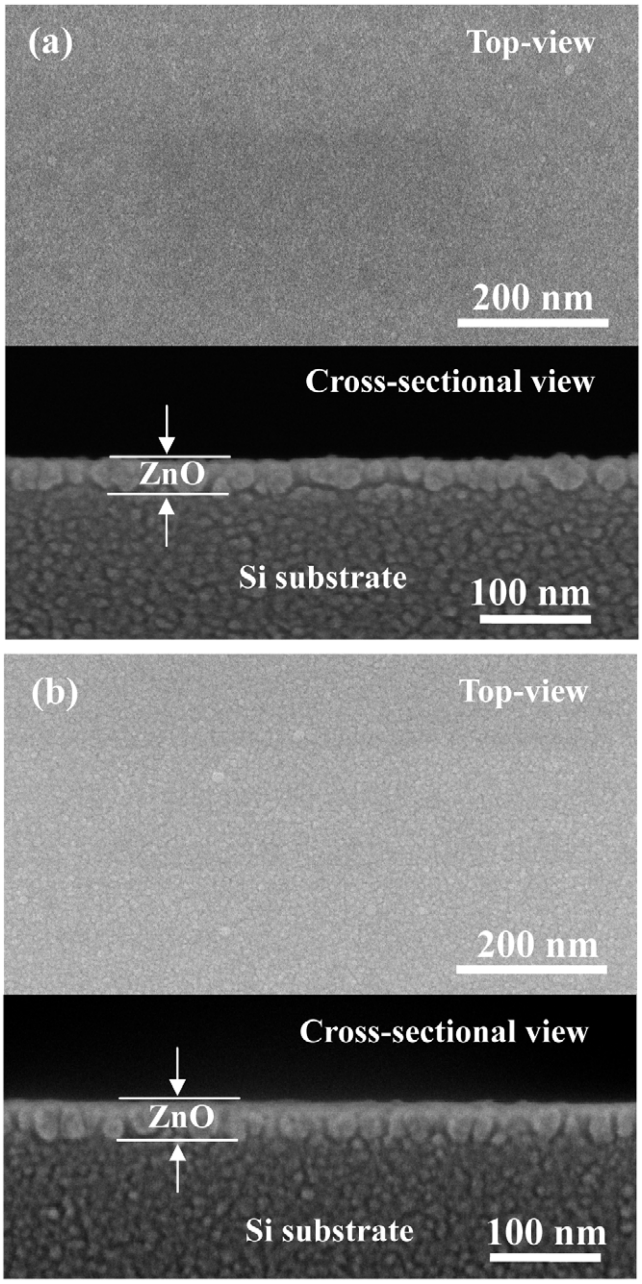

Figure 7. Top and cross-sectional SEM micrographs for ZnO thin films subjected to annealing at (a) 200 °C and (b) 500 °C for 2 h.

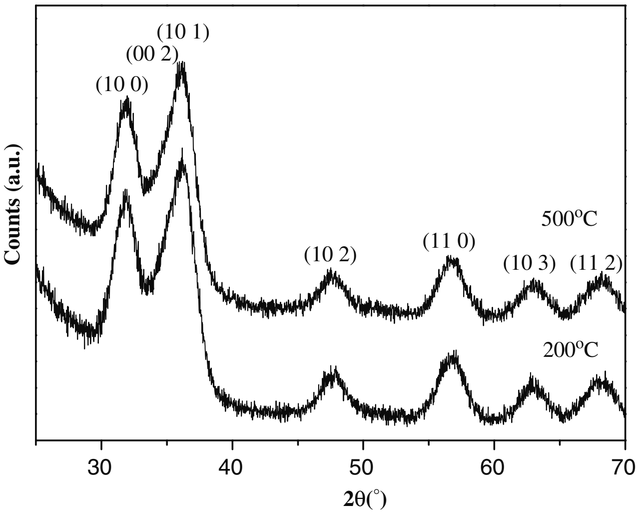

Figure 8. XRD patterns of ZnO layers annealed at 200 and 500 °C for 2 h.

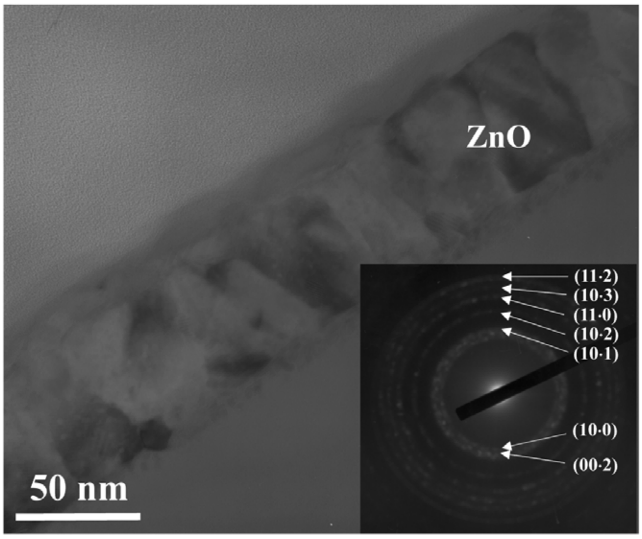

Figure 9. High-magnification, cross-sectional TEM images of ZnO thin film subjected to annealing at 500 °C for 2 h. The inset picture at the lower right-hand side is the SAED pattern taken in the vicinity of the ZnO layer.

clearly reveals that the ZnO nanoparticles with an initial size as small as 5 nm coalescence into granules 50 nm in size, about equal to the thickness of the deposited layer, via annealing at 200 °C. This is ascribed to the high specific-surface-area (SSA) feature of nano-scale ZnO particles that is able to ignite the grain growth of ZnO at such a low annealing temperature. As to the sample subjected to 500 °C annealing, the ZnO grain size remains the same at about 50 nm. This is due to the thermal grooving effect; the equilibrium of surface tensions at the ambient/ZnO interface impede the grain boundary migration and hence limits further enlargement of the grain size in the ZnO layer. Furthermore, there is no dramatic change in the thickness of the ZnO layer when the annealing temperature is raised from 200 to 500 °C due to the relatively fast grain growth at temperatures as low as 200 °C.

Figure 8 depicts the XRD patterns of ZnO layers annealed at 200 and 500 °C for 2 h. The nearly identical shape of the XRD profiles implies no significant change in the grain structure of the ZnO layers subjected to different annealing treatments, iterating the fast grain growth and thermal grooving effect in the ZnO layers presented above.

Figure 9 presents high-magnification, cross-sectional TEM images of the ZnO layer on Si substrate subjected to annealing at 500 °C for 2 h. The ZnO grain size deduced by TEM is in essence the same as that obtained by SEM reported above. In conjunction with selected area electron diffraction (SAED) analysis, TEM characterization also shows that the

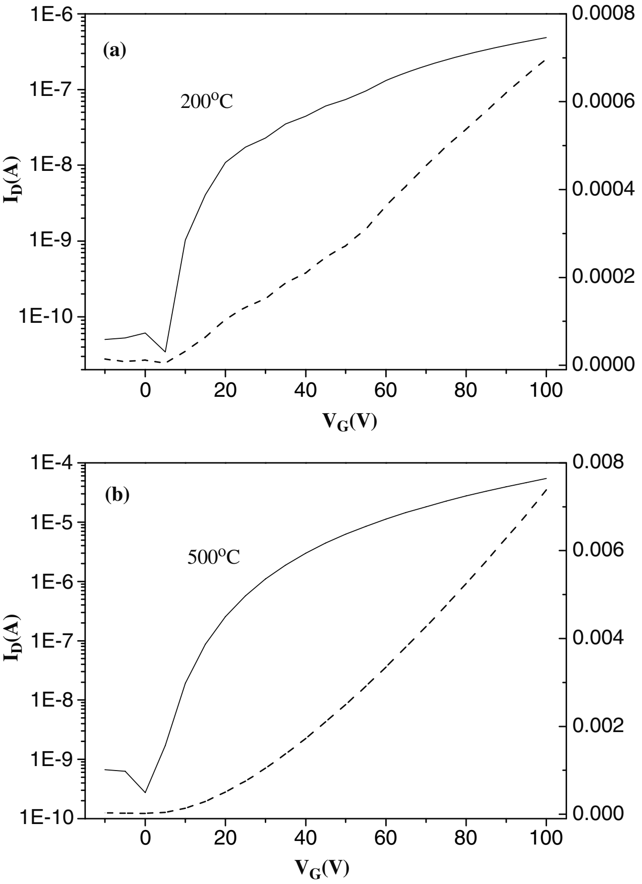

Figure 10. Transfer characteristics of TFT samples subjected to annealing at (a) 200 °C and (b) 500 °C for 2 h.

ZnO grains align in a random manner, i.e., the absence of *c*-axis texture as observed in sputtering deposited ZnO layers.

3.3. Characterization of ZnO TFT devices

Figures 10(a) and (b) show the transfer characteristics of 50 nm thick ZnO TFT samples subjected to annealing at 200 °C and 500 °C for 2 h, respectively. The key electrical properties of ZnO TFT samples subjected to the annealing treatments at temperatures ranging from 200 to 500 °C for 2 h are summarized in table 1. The device subjected to 200 °C annealing exhibits on/off ratio $= 10^4$, threshold voltage (V_{th}) $= 16.8$ V and $\mu = 0.0009$ cm^2 V^{-1} s^{-1} while the sample subjected to 500 °C annealing possesses on/off ratio $= 10^5$, $V_{\mathrm{th}} = 17.1$ V and $\mu = 0.104$ cm^2 V^{-1} s^{-1}. The improvement of the electrical performance with the increase of annealing temperature confirms the results of TGA and FT-IR analyses. It is attributed to the removal of the hydroxyl group and GPTS residing on the ZnO nanoparticles that may cause the scattering during charge carrier transport. We note that the V_{th}s remain at 16.5–17.5 V even though the annealing temperature is raised up to 500 °C. The unceasing V_{th} is attributed to the presence of grain boundaries in ZnO thin films which form the double Schottky barrier and thus block the electron transport in polycrystalline ZnO thin film [21]. Further, the nano-scale ZnO grain size causes an increase of the conduction band edge and further departs from the Fermi energy level (E_{f}). This may also deteriorate the electrical properties of TFT devices. The above results indicate, for solution processes utilizing precursor solutions containing nanoparticles, innovations on the post-annealing method that may effectively eliminate the grain boundaries in ZnO films would be a key issue for further improvement of the electrical properties of TFT devices.

Table 1. Electrical properties of ZnO TFT devices subjected to annealing treatments at temperatures ranging from 200 to 500 °C for 2 h.

Temperature (°C)	V_{th} (V)	μ (cm^2 V^{-1} s^{-1})	On/off ratio
200	16.8	0.0009	10^4
300	17.0	0.0083	10^4–10^5
400	17.2	0.0235	10^4–10^5
500	17.1	0.1040	10^5

4. Conclusions

In summary, we prepared nano-scale ZnO particles and adopted GPTS to modify the ZnO nanoparticles so as to form a highly stable ZnO precursor solution for solution processing of TFT devices. Analytical results showed that GPTS is an effective chemical dispersant to stabilize the ZnO nanoparticles in EG solvent and it is able to form highly uniform, nearly pore-free ZnO layers via a spin coating process in conjunction with an appropriate post-annealing treatment. Further, the high SSA feature of ZnO nanoparticles with an initial size of about 5 nm was found to promote grain growth in the ZnO layer at temperatures as low as 200 °C. Although transfer characteristics were observed in the 200 °C-annealed ZnO TFT sample, the incomplete removal of the hydroxyl group and GPTS residing on ZnO nanoparticles deteriorated the device performance. By escalating the annealing temperature to 500 °C, a TFT sample with satisfactory electrical properties, on/off ratio $= 10^5$, $V_{\mathrm{th}} = 17.1$ V and $\mu = 0.104$ cm^2 V^{-1} s^{-1}, could be obtained. However, the relatively high V_{th} indicates that innovations on the post-annealing method to eliminate the grain boundaries in ZnO films are still required for further improvement of the electrical properties of TFT devices prepared by solution processes.

Acknowledgments

This work is supported by the National Science Council (NSC), Taiwan, ROC, under contract No. NSC96-2221-E-009-010. TFT device characterization supported by Printing Science Department at Display Technology Center (DTC), Industrial Technology Research Institute (ITRI), Taiwan, ROC, is also deeply acknowledged.

References

[1] Hoffman R L, Norris B J and Wager J F 2003 *Appl. Phys. Lett.* **82** 733
[2] Pauporte T, Jouanno E, Pelle F, Viana B and Aschehoug P 2009 *J. Phys. Chem.* C **113** 10422

[3] Ni M, Leung M K H, Leung D Y C and Sumathy K 2006 *Sol. Energy Mater. Sol. Cells* **90** 2000

[4] Minami T 2005 *Semicond. Sci. Technol.* **20** S35

[5] Bao Z, Dodabalapur A and Lovinger A J 1996 *Appl. Phys. Lett.* **69** 4108

[6] Garnier F, Hajlaoui R, Kassmi A E, Horowitz G, Laigre L, Porzio W, Armanini M and Provasoli F 1998 *Chem. Mater.* **10** 3334

[7] Okamura K, Mechau N, Nikolova D and Hahn H 2008 *Appl. Phys. Lett.* **93** 083105

[8] Sun B, Peterson R L, Sirringhaus H and Mori K 2007 *J. Phys. Chem.* C **111** 18831

[9] Schneider J, Hoffmann R C, Engstler J, Soffke O, Jaegermann W, Issanin A and Klyszcz A 2008 *Adv. Mater.* **20** 3383

[10] Sun B and Sirringhaus H 2005 *Nano Lett.* **5** 2408

[11] Ong B S, Li C S, Li Y N, Wu Y L and Loutfy R 2007 *J. Am. Chem. Soc.* **129** 2750

[12] Meulenkamp E A 1998 *J. Phys. Chem.* B **102** 5566

[13] Mikrajuddin, Lenggoro I W, Okuyama K and Shi F G 2002 *J. Electrochem. Soc.* **149** H107

[14] Huang H C and Hsieh T E 2010 *Ceram. Int.* **36** 1245

[15] Hung C H and Whang W T 2005 *J. Mater. Chem.* **15** 267

[16] Kagan C R and Andry P 2003 *Thin Film Transistors* (New York: Dekker)

[17] Sakohara S, Ishida M and Anderson M A 1998 *J. Phys. Chem.* B **102** 10169

[18] Yadav H K, Sreenivas K, Gupta V, Singh S P and Katiyar R S 2007 *J. Mater. Res.* **22** 2404

[19] Shang X Y, Zhu Z K, Yin J and Ma X D 2002 *Chem. Mater.* **14** 71

[20] Morrison I D 2002 *Colloidal Dispersions: Suspensions, Emulsions, and Forms* (New York: Wiley-Interscience)

[21] Hossain F M, Nishii J, Takagi S, Ohtomo A, Fukumura T, Fujioka H, Ohno H, Koinuma H and Kawasaki M 2003 *J. Appl. Phys.* **94** 7768